

Colored Percolation

Sumanta Kundu and S. S. Manna

Satyendra Nath Bose National Centre for Basic Sciences, Block-JD, Sector-III, Salt Lake, Kolkata-700106, India

A model named ‘Colored Percolation’ has been introduced with its infinite number of versions in two dimensions. The sites of a regular lattice are randomly occupied with probability p and are then colored by one of the n distinct colors using uniform probability $q = 1/n$. Denoting different colors by the letters of the Roman alphabet, we have studied different versions of the model like $AB, ABC, ABCD, ABCDE, \dots$ etc. Here, only those lattice bonds having two different colored atoms at the ends are defined as connected. The percolation thresholds $p_c(n)$ asymptotically converges to its limiting value of p_c as $1/n$. The model has been generalized by introducing a preference towards a subset of colors when m out of n colors are selected with probability q/m each and rest of the colors are selected with probability $(1 - q)/(n - m)$. It has been observed that $p_c(q, m)$ depends non-trivially on q and has a minimum at $q_{min} = m/n$. In another generalization the fractions of bonds between similar and dissimilar colored atoms have been treated as independent parameters. Phase diagrams in this parameter space have been drawn exhibiting percolating and non-percolating phases.

I. INTRODUCTION

Over the last several decades, the phenomenon of percolation has been proved to be one of the most investigated models in the topic of transport in random disordered systems [1–6]. Broadbent and Hammersley first introduced the model of percolation trying to better understand the mechanism of fluid flow through a random porous medium [7], and now it has become one of the simplest models of studying order-disorder phase transition [8]. Due to its simplicity and plenty of applicability in a number of fields, the literature on this topic is vast and expectedly a large number of variants of percolation models have been introduced to study the critical behaviors of widely different systems [6, 9–16]. In particular, the percolation theory has been successfully applied to the well known sol-gel transition [17], transitions in conductor-insulator mixtures using the random resistor networks [18, 19], propagation of fires in the forests [1, 20], spreading of infectious diseases in the form of epidemics [21, 22], etc.

In the ordinary percolation, the sites of a regular lattice are occupied randomly and independently with probability p or kept vacant with probability $(1 - p)$. Any two adjacent occupied sites are considered as connected. A group of such occupied sites interconnected through their neighboring connections forms a cluster, the properties of which depend on p . At any arbitrary value of p , there are several clusters of different shapes and sizes. The size of the largest cluster increases monotonically as p is increased and right above a critical value of $p = p_c$, known as the percolation threshold, the largest cluster includes sites on the opposite sides of the lattice and thus for the first time a global connectivity is established. Therefore, p_c marks the transition point, between the globally connected and disconnected phases, characterized by the divergence of the correlation length $\xi(p)$ as $p \rightarrow p_c$. It is well known that the ordinary percolation undergoes a continuous phase transition at $p = p_c$ and the set of critical exponents defined at and around p_c characterizes the

universality class of the transition [1]. The best known value of $p_c(\text{sq})$ for the site percolation on the square lattice is 0.59274605079210(2) [23] and $1/2$ for the bond percolation [24].

Inspired by the phenomena of anti-ferromagnetism, gelation, spreading of infection from the infected cells to normal cells, Mai and Halley introduced the AB percolation model [2, 25–27]. The model of AB percolation is illustrated in the following way. Initially, all sites of a lattice are occupied with B atoms. Then, random sites are selected one by one and the B atoms at these sites are replaced by the A atoms. At any arbitrary intermediate stage the fraction of A atoms is denoted by r . According to this model, bonds which are having both A and B atoms at their opposite ends are marked connected. For a given value of r , the probability that any given edge has a bond is $2r(1 - r)$, which has its maximum at $r = 1/2$ and decreases monotonically on both sides of this point. Consequently, the average size of the largest cluster gradually grows till $r = 1/2$. The entire scenario is symmetric about $r = 1/2$. At $r = 1 - r_c$, the size of the largest cluster drops sharply, and finally it vanishes at $r = 1$. Therefore, for $r_c \leq r \leq 1 - r_c$, the system is percolating. However, the existence of a global connectivity through the alternating A and B atoms and therefore the existence of r_c , crucially depends on the geometry of the underlying lattice [27, 28]. For example, spanning AB cluster does not exist on the square lattice [28, 29], but it exists on the triangular lattice [30]. Although, it was first concluded that the universality class of AB percolation in two dimensions is different from the ordinary percolation [26], later it has been argued that it belongs to the same universality class as the ordinary percolation [31–33]. Further, random occupation of lattice sites by more than two distinct atoms was studied through the model of polychromatic percolation [34, 35].

In this paper, we consider a percolation model, where the sites of a regular lattice are occupied with probability p similar to the ordinary site percolation, and then at every occupied site one of the n different colored atoms

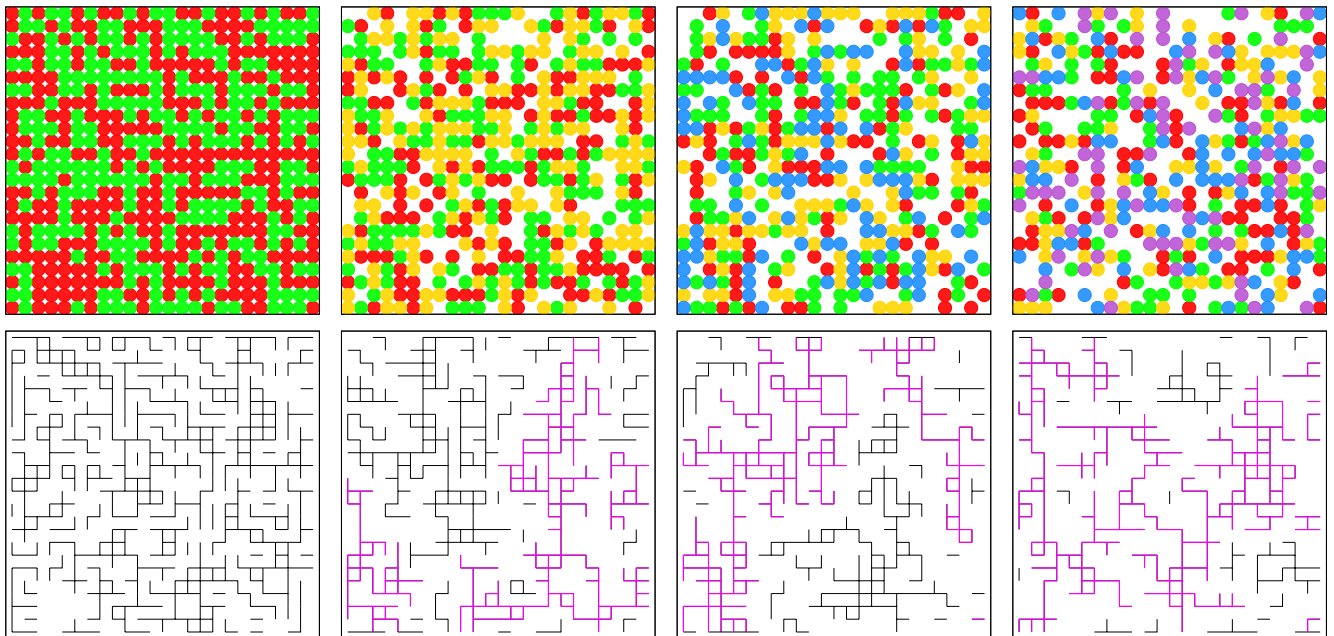


FIG. 1: Typical configurations of AB, ABC, ABCD, and ABCDE percolation (from left to right) at their critical points have been shown on a 24×24 square lattice with periodic boundary conditions along the horizontal direction. The colors used are: red (*A*), green (*B*), yellow (*C*), blue (*D*) and orchid (*E*) and are distributed with uniform probabilities. The corresponding bond configurations with the spanning clusters painted in magenta have been shown in the lower panel. It may be noted that for *AB* percolation, there is no spanning cluster even when all the sites are occupied.

is assigned with a given probability q . A bond between a pair of neighboring occupied sites is declared as connected if the atoms are of different colors. We refer this model as the colored percolation. We study the critical properties of this model for both the square and triangular lattices.

The paper is organized as follows. We start by describing the model of colored percolation in Sec. II, where we consider every color to be equally likely. In Sec. III, we generalize the model by introducing a preference towards the selection of a subset of colors and its simulation results. Percolation transition using similarly colored bonds in addition to the dissimilar bonds has been described in Sec. IV. Percolation transition mixing the fractions of similarly and dissimilarly colored bonds are reported in Sec. V. The critical properties of the model are presented in Sec. VI. Finally, we summarize in Sec. VII.

II. MODEL

The sites of a $L \times L$ regular and initially empty lattice are occupied randomly by atoms one by one. At any arbitrary stage, the density of atoms is denoted by p . After occupying a given site, the corresponding atom is colored by selecting one of the n colors with probability $q = 1/n$. The letters of the Roman alphabet are used to denote the different colors. The bonds, which have two distinct colored atoms at their opposite ends, are

declared as connected. Therefore, the other bonds having same colored atoms like *AA*, *BB* etc., are not connected. Gradually, the number of connected bonds in the system increases with increasing the value of p .

For $n = 2$, every selected site is occupied either by a *A* atom or by a *B* atom with probability $q = 1/2$. Like the model of *AB* percolation, the size of the largest cluster never assumes a macroscopic size on the square lattice and therefore, a percolation transition is absent here. On the other hand, our simulation results indicate that on the triangular lattice the percolation transition occurs at $p_c \approx 0.729$.

For $n = 3$, every selected site is occupied by one of the three atoms *A*, *B*, and *C* with probabilities $q = 1/3$. Only the *AB*, *BC*, and *CA* bonds are defined to be connected. In this case, there exists a percolation threshold $p_c \approx 0.807$ on the square lattice and ≈ 0.630 on the triangular lattice. We refer this model as *ABC* percolation.

Such an extension of the model can be continued with four colored atoms, where *A*, *B*, *C*, and *D* atoms are distributed with probabilities $q = 1/4$. The critical densities of the occupied sites are $p_c \approx 0.734$ on the square lattice and ≈ 0.591 on the triangular lattice estimated using the method in [36]. This model is referred as the *ABCD* percolation.

We systematically increase the number of distinct colored atoms to define further the *ABCDE*, *ABCDEF*, *ABCDEFGH* etc., colored percolation models. In brief, we have been able to define an infinite set of percolation models by defining con-

nectivity through the bonds between dissimilar atoms. Figure 1 shows the images of the typical percolation configurations on the square lattice for four different values of n .

A. The Order Parameter and the Percolation Threshold

The size of the largest cluster for a particular value of p and for the system of size L is denoted by $s_{max}(p, L)$ and the average fractional size of the largest cluster is defined as the order parameter $\Omega(p, L) = \langle s_{max}(p, L) \rangle / L^2$. The variation of $\Omega(p, L)$ with p has been shown in Fig. 2(a) for six different values of n on the square lattice. The sharp rise in the order parameter curve shifts towards smaller values of p with increasing the value of n .

As p is increased, the size of the largest cluster increases monotonically by merging with the other clusters, whereas the variation of the second largest cluster is not monotonic. In a typical run α , the second largest cluster may merge several times with the largest cluster and thereby causes multiple jumps in the size of the largest cluster. At a specific value of p , the maximum of the second largest cluster merges with the largest cluster that results the maximal jump in the size of the largest cluster. This particular value of p is defined as the percolation threshold p_c^α for the run α [36, 37]. For a fixed value of n , this calculation is repeated over a large number of independent runs α and the p_c^α values are averaged to obtain $p_c(n, L) = \langle p_c^\alpha \rangle$ for the system size L . In our simulation, periodic boundary conditions are imposed along both the vertical and horizontal directions. The value of $s_{max}(p, L)$ is evaluated using the algorithm given in reference [38] over the entire range of p .

For a given value of n , the $p_c(n, L)$ values are extrapolated using Eqn. 1,

$$p_c(n, L) = p_c(n) - AL^{-1/\nu} \quad (1)$$

to obtain the asymptotic value of the percolation threshold $p_c(n)$ for $L \rightarrow \infty$, where ν is known as the correlation length exponent. Using $1/\nu$ as a free parameter we varied it's trial values at the interval of 0.001 and found by the least square fitting method that the best values for all n differ from $3/4$ by at most 0.005. Therefore in the rest of our calculation we have used $\nu = 4/3$, the exact value of the exponent in two dimensions [1, 39]. In Fig. 2(b), we plot $p_c(n, L)$ against $L^{-1/\nu}$ in a linear scale for six different values of n . The data points for all six values of n fits excellently to a straight line. By extrapolating the straight lines as $L \rightarrow \infty$ and measuring the y -intercept we estimate the asymptotic values of $p_c(n)$. The values of $p_c(n)$ for first few values of n are listed in Table I for square and triangular lattices. It is to be noted that, for each value of n , the $p_c(n, L)$ values are calculated numerically using $L = 64, 128, 256, 512, 1024$, and 2048.

As the number of different colors increases, there are more and more connected bonds in the system which

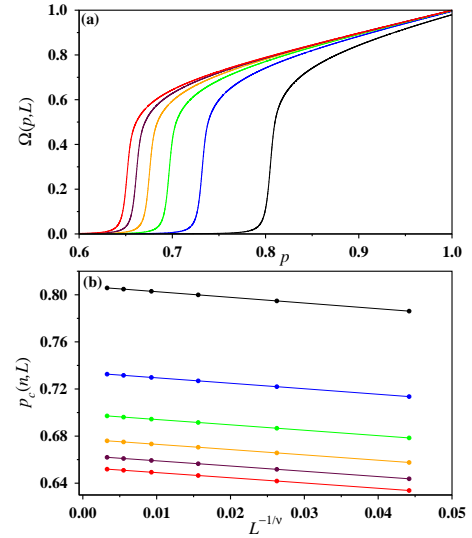


FIG. 2: For $n = 3$ (black), 4 (blue), 5 (green), 6 (orange), 7 (maroon), and 8 (red): (a) the order parameter $\Omega(p, L)$, has been plotted against the site occupation probability p for the square lattice of size $L = 1024$ (n increases from right to left); (b) plot of the percolation thresholds $p_c(n, L)$ against $L^{-1/\nu}$ using $\nu = 4/3$ (n increases from top to bottom). By extrapolating as $L \rightarrow \infty$, we obtain the asymptotic values of the percolation threshold $p_c(n)$.

helps the system to percolate at smaller densities. The probability that a bond would be a connected one is given by $p_b = 1 - 1/n$ and therefore, for very large value of n the entire scenario is exactly same as the ordinary site percolation. Expectedly, $p_c(n)$ approaches towards $p_c = p_c(\infty)$, the ordinary site percolation threshold on the corresponding lattice.

To investigate how the asymptotic values of the percolation threshold $p_c(n)$, approach to the value p_c as $n \rightarrow \infty$, we first calculate $p_c(n)$ for different values of

n	$p_c(n)$	
	Square	Triangular
2		0.72890(4)
3	0.80745(5)	0.63005(4)
4	0.73415(4)	0.59092(3)
5	0.69864(7)	0.56991(5)
6	0.67751(5)	0.55679(5)
7	0.66345(5)	0.54782(3)
8	0.65342(8)	0.54130(3)
9	0.64588(5)	0.53634(2)
10	0.64002(4)	0.53245(3)
11	0.63532(5)	0.52931(2)
12	0.63147(4)	0.52672(2)

TABLE I: Numerical estimates of the asymptotic values of the percolation threshold $p_c(n)$ for n different colored atoms occur with probability $1/n$ for the square and triangular lattice geometries.

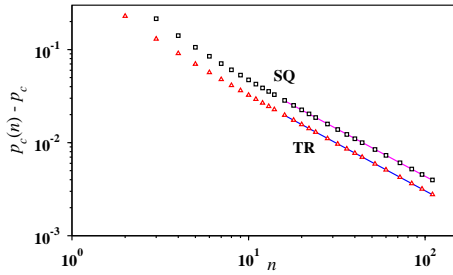


FIG. 3: Plot of $p_c(n) - p_c$ against n (upto $n = 110$) on a log-log scale, using $p_c = p_c(\text{sq})$ and $1/2$ for the square and triangular lattices respectively. The slope of the curves in the fitted regime have been found to be 1.020 and 1.017 respectively.

n upto $n = 110$. Then, we plot the deviation $p_c(n) - p_c$ against n on a double logarithmic scale for the square and triangular lattices (Fig. 3). Although both the curves have curvatures at their initial regimes, for large values of n they are quite straight. The slopes of the curves within a window ranges between $n = 16$ and 110 measured as 1.020 and 1.017 for the square and triangular lattices respectively. We observed that these slopes approach gradually to a value unity as we shift the window to higher values of n . Thus, we conjecture that $p_c(n) - p_c \sim n^{-1}$ for both the lattices.

III. PREFERENTIAL COLORED PERCOLATION

A straightforward generalization of this model can be achieved by introducing a preference towards the probability of selection of different colored atoms. In the simplest case, let us consider the atoms of color C to be preferentially selected whereas all other colored atoms are on the same footing. More specifically, we denote the probability of selection of the C atoms by q and for all other atoms it is $(1 - q)/(n - 1)$. As before, only the bonds between dissimilar atoms are defined to be connected.

For a given value of q , if Prob_{ii} is the probability that two atoms at the end sites of a bond are of same color i , then the probability that a particular bond would be a connected one is given by,

$$\text{Prob}_b(q) = 1 - \sum_{i=1}^n \text{Prob}_{ii} = 1 - q^2 - (1 - q)^2/(n - 1). \quad (2)$$

The above expression describes that with increasing the value of q from 0, the $\text{Prob}_b(q)$ first increases, reaches its maximum at $q = q_{\min}$ and finally decreases beyond this point. The condition $d\text{Prob}_b(q)/dq = 0$ at $q = q_{\min}$ yields the value of $q_{\min} = 1/n$. This property of $\text{Prob}_b(q)$ should be reflected in the percolation properties of the system also. Consequently, the percolation threshold $p_c(q)$ must decrease with q , till it reaches q_{\min} and then increase for $q > q_{\min}$.

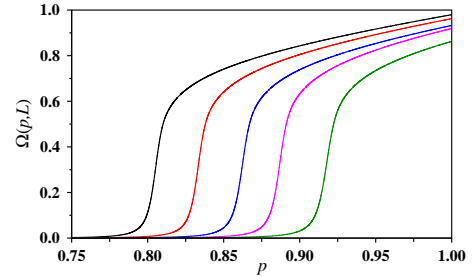


FIG. 4: Plot of the order parameter $\Omega(p, L)$ against occupation probability p for the preferential ABC percolation on square lattice of size $L = 1024$. The values of q are $1/3$ (black), 0.20 (red), 0.53 (blue), 0.12 (magenta), and 0.60 (green) arranged from left to right.

For $n = 3$, the variations of the order parameter for different values of q have been shown in Fig. 4. For $q = 0$, one gets back the $n = 2$ unpreferred colored percolation, and therefore, for the square lattice even a fully occupied lattice does not percolate. Further, on increasing the value of q the BC and CA bonds are created which eventually also contribute to the global connectivity. Tuning the value of q , it has been observed that there exists a threshold value of $q = q_1$ when the global connectivity first appears, i.e., $p_c(q_1) = 1$. If the probability q is increased further, the percolation threshold $p_c(q)$ gradually decreases and reaches to its minimum value $p_c(q_{\min}) \approx 0.807$ at $q_{\min} \approx 0.333$. On increasing q even further, $p_c(q)$ increases and reaches the value of unity again at $q = q_2$. The global connectivity is lost beyond this point. For each value of q , first the percolation threshold $p_c(q, L)$ for the system size L is estimated for $L = 256, 512$ and 1024 and then they are extrapolated as $L \rightarrow \infty$ using Eqn. (1) to obtain $p_c(q)$. The variation of $p_c(q)$ for the entire range of q has been shown in Fig. 5.

For the triangular lattice, the curve retains its shape but in this case, even for $q = 0$, there exists a percolation threshold. Since, for $q = 0$ the other two atoms are occupied with probability $1/2$, the value of percolation threshold is expected to be ≈ 0.729 . Similarly, for $q = 0$ and $n = 4$ on the square lattice this model is identical to the ABC percolation and therefore, $p_c(0) \approx 0.807$.

Numerically, the values of q_1 and q_2 are determined using the bisection method in the following way. To estimate q_2 , we select a pair of values q^c and q^d for q so that the system is globally connected and disconnected respectively for $p = 1$. We have applied the periodic boundary condition along one direction and tested for the global connectivity along its transverse direction using the Burning algorithm [40] for $q = (q^c + q^d)/2$. If the system is globally connected then q^c is replaced by q , otherwise q^d is replaced by q . This procedure is repeated until $q^d - q^c < 10^{-7}$, when $(q^c + q^d)/2$ defines q_2 for a particular run. Averaging over a large number of independent runs $q_2(n, L)$ for specific values of n and L

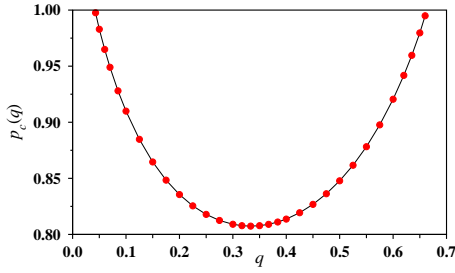


FIG. 5: For the preferential *ABC* percolation on the square lattice, percolation threshold $p_c(q)$ is plotted against the parameter q . The minimum of $p_c(q)$ occurs at $q = 0.333$ which is in agreement with its estimate of $1/3$, using Eqn. (2).

has been estimated. Similar procedure has been followed for $q_1(n, L)$. The entire procedure is then repeated for different values of L and extrapolations to $L \rightarrow \infty$ using Eqn. (1) in this case as well, we obtain $q_1(n)$ and $q_2(n)$. For $n = 3$, the best linear fit has been exhibited in Fig. 6 by plotting $q_2(3, L) - q_2(3)$ against $L^{-0.740}$, using $q_2(3) = 0.6639(5)$ on the square lattice. Similarly, $q_1(3) = 0.0414(5)$ has been estimated.

Therefore, a non-trivial value of $q_1(n)$ exists for $n = 2$ on the square lattice. It does not exist for all other values of n on the square lattice and for all values of n on the triangular lattice. On the other hand, $q_2(n)$ exists for both the lattices and for all values of n .

The density of connected bonds $\text{Prob}_b(q)$ corresponding to the point $q = q_2(n)$ represents a threshold value in the correlated bond percolation scenario. Beyond this point, the density of connected bonds is no longer sufficient to establish a global connectivity. Neglecting the local correlations and equating $\text{Prob}_b(q_2)$ to p_c^b , the random bond percolation threshold of the respective lattices, we arrive at an expression of $q_2(n)$ using Eqn. (2),

$$q_2(n) = \left[1 + [1 + n[(1 - p_c^b)(n - 1) - 1]]^{1/2} \right] / n. \quad (3)$$

Numerically estimated values of $q_2(n)$ for different val-

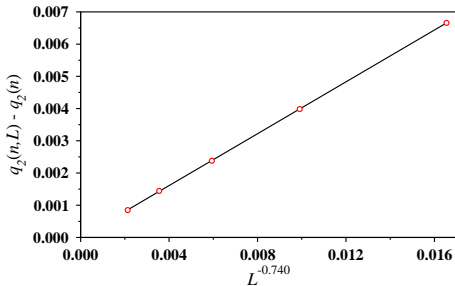


FIG. 6: For $n = 3$ and for square lattice, plot of $q_2(n, L) - q_2(n)$ against $L^{-0.740}$ with $q_2(n) = 0.6639$ exhibits an excellent straight line which passes very close to the origin. The value of $q_2(n, L)$ is calculated for $L = 256, 512, 1024, 2048$ and 4096 .

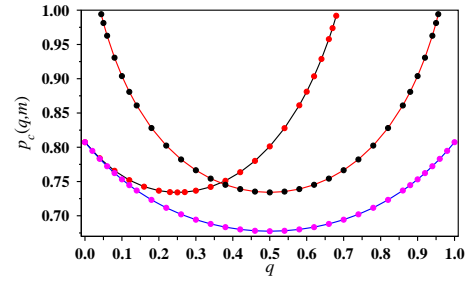


FIG. 7: The variation of the percolation threshold $p_c(q, m)$ with q for the generalized version of the preferential colored percolation model is shown for $m = 1, n = 4$ (black); $m = 2, n = 4$ (red); and $m = 3, n = 6$ (blue) for the square lattice. The curves are arranged from top to bottom along the line $q = 0.50$.

ues of n using bisection method, along with the values obtained from Eqn. (3) using $p_c^b = 1/2$, are summarized in Table II for the square lattice. It is observed that the values are close to each other and differ only due to the existence of short range correlations in the system.

A more general version of the preferential colored percolation model is the situation when m distinct colored atoms are equally probable and the remaining $(n - m)$ colors are also equally probable but occur with different probabilities. Such a generalization can be obtained by assigning an atom of one of the m colors with probability q/m and rest of the $(n - m)$ colors with probability $(1 - q)/(n - m)$ at the time of occupying a vacant site. The probability for an arbitrary bond to be connected is given by,

$$\text{Prob}_b(q, m) = 1 - q^2/m - (1 - q)^2/(n - m). \quad (4)$$

Evidently, $\text{Prob}_b(q, m)$ is maximum at $q_{min} = m/n$ and it decreases on both sides of this point. The expression of $\text{Prob}_b(q, m)$ remains unaltered if the value of q is changed from q to $(1 - q)$ at the same time m is changed from m to $(n - m)$, i.e., $\text{Prob}_b(q, m) = \text{Prob}_b(1 - q, n - m)$. Immediately, it implies that the curve is symmetric about $q = 1/2$ only when $m = n/2$. The percolation threshold $p_c(q, m)$ for specific values of n and m is expected to exhibit such properties appropriately.

Again, after extrapolation to the large L limit using

n	3	4	5	6	7	8
Numerical	0.6639	0.6849	0.6927	0.6969	0.6995	0.7013
Analytical	2/3	0.6830	0.6899	0.6937	0.6961	0.6978

TABLE II: The comparison of $q_2(n)$, evaluated using Eqn. (3) with its numerical estimates for different values of n for square lattice. For each values of n , numerically $q_2(n, L)$ is calculated for $L = 256, 512, 1024, 2048$, and 4096 and on extrapolation to $L \rightarrow \infty$ we obtained $q_2(n)$. Each of the reported value has an error bar of 5 in the last digit.

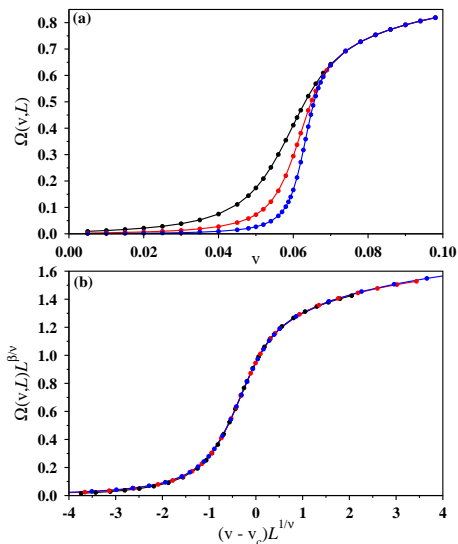


FIG. 8: (a) For $L = 256$ (black), 512 (red) and 1024 (blue) (arranged from left to right), the order parameter $\Omega(v, L)$ has been plotted with the bond occupation probability v between AA or BB atoms at $p = 1$, for $n = 2$ with $q = 1/2$ colored percolation. (b) By suitably scale the abscissa and ordinate when the same data as in (a) is replotted, a nice data collapse is observed using $v_c = 0.0651$, $\beta/\nu = 0.101(5)$ and $1/\nu = 0.745(5)$.

Eqn. (1) with $\nu = 4/3$ we obtain $p_c(q, m)$. In Fig. 7, the asymptotic values of the percolation threshold $p_c(q, m)$ have been plotted against q for three pairs of values of m and n for the square lattice. It is observed that all three curves have their own minimum which occur at $q_{min} = 0.25, 0.50$ and 0.50 for $m = 1, n = 4$; $m = 2, n = 4$; and $m = 3, n = 6$ respectively. Clearly, the q_{min} values match excellently with our analytically estimated value of $q_{min} = m/n$. As expected, the curves corresponding to $m = n/2$ are symmetric about the point $q = 1/2$.

IV. PERCOLATION USING ADDITIONAL SIMILAR BONDS

Let us recall that for $n = 2$ case on the square lattice and for any arbitrary value of the site occupation probability p , the density of AB bonds is maximum for $q = 1/2$. In spite of that no percolation transition is observed on the square lattice since the largest cluster of AB bonds is found to be minuscule even when $p = 1$. In other words, even the maximum number of connected bonds are not sufficient to establish a global connectivity across the system [28].

In this section we study a new variant of our colored percolation model, where in addition to the AB bonds, we allow also a fraction v of similarly colored bonds (like AA and BB) to be connected. Therefore, for $v = 1$, the problem reduces to the ordinary site percolation with the

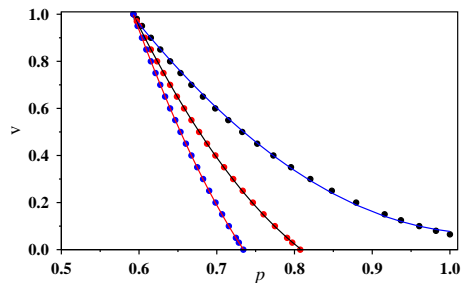


FIG. 9: Phase diagram of the density v of similarly colored bonds and the site occupation probability p for $n = 2$ (black), 3 (red), and 4 (blue) (arranged from right to left) with $q = 1/n$. The critical curve is fitted very closely by the Eqn. 6 whose parameters are $c_1 = 5.01, 8.28$, and 11.47 ; $c_2 = -9.48, -17.92$, and -26.25 ; $c_3 = 4.55, 9.50$, and 14.47 for $n = 2, 3$, and 4 respectively.

percolation threshold at $p_c(\text{sq})$. This suggests that for all values of $p_c(\text{sq}) \leq p \leq 1$ there should be a critical value of $v = v_c(p)$ for the fraction of bonds between similarly colored atoms, such that percolation transition occurs only for $v \geq v_c(p)$.

For $p = 1$ one must include a non-trivial fraction $v_c(1)$ of similar bonds to achieve a percolation transition. On a fully occupied lattice we have used again the bi-section method to obtain an accurate estimation of $v_c(1)$. Starting with two trial values of v corresponding to the globally connected and unconnected systems, the gap between them is reduced by successive halving of the interval. As before, the values of $v_c(1, L)$ obtained this way have been extrapolated for $L \rightarrow \infty$ to obtain $v_c(1) = 0.0651(5)$. It may be noted that the existence of a non-zero value of $v_c(1)$ is a numerical demonstration of the absence of a percolation transition in the $n = 2$ colored percolation as well as in the AB percolation on the square lattice.

In Fig. 8(a), the order parameter $\Omega(v, L) = \langle s_{max}(v, L) \rangle / L^2$ has been plotted against v for three different sizes of the system. For $v = 0$, only the AB bonds are present in the system and the size of the largest cluster is minuscule, which is apparent by the very small value of the order parameter. On increasing v further, the order parameter grows monotonically and the sharpest rise occurs at a critical value $v_c(1, L)$ leading to the occurrence of global connectivity. A finite-size scaling analysis is exhibited in Fig. 8(b) indicating a scaling form:

$$\Omega(v, L)L^{\beta/\nu} \sim \mathcal{F}[(v - v_c(1))L^{1/\nu}]. \quad (5)$$

Using $v_c = 0.0651$, the best data collapse is observed for $1/\nu = 0.745(5)$ and $\beta/\nu = 0.101(5)$, compared to the exact value of the correlation length exponent $1/\nu = 3/4$ and $\beta/\nu = 5/48 \approx 0.104$ for the ordinary percolation in two dimensions [1]. In addition, our estimates for the fractal dimension $d_f = 1.896(5)$ of the infinite incipient cluster [41] and the exponent $\gamma = 2.388(5)$ of the second moment of the cluster size distribution at $v_c(1, L)$ yield

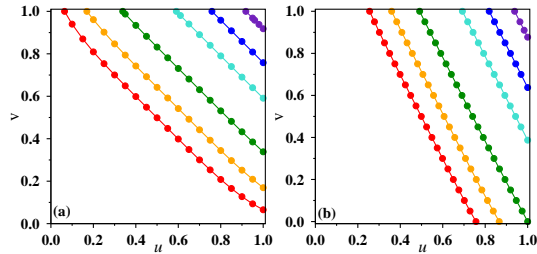


FIG. 10: Phase diagram of the density of similarly colored bonds v and dissimilarly colored bonds u for fixed values of p for $n = 2$ (a) and $n = 3$ (b), with $q = 1/n$ using $L = 1024$ on the square lattice. The values of p are 1.00 (red), 0.90 (orange), 0.80 (green), 0.70 (cyan), 0.65 (blue), and 0.61 (indigo) (arranged from left to right). For every p , the region above the critical curve depicts the percolating phase.

values very much consistent with the exactly known exponents of $d_f = 91/48$ and $\gamma = 43/18$ for the ordinary percolation which fulfill the scaling and hyperscaling relations in two dimensions: $\gamma/\nu + 2\beta/\nu = 2$ [1, 42].

Repeating this method for many different values of occupation probability p we have drawn the phase diagram in the $v-p$ plane in Fig. 9. This plane is divided into two regions by the critical curve $v_c(p) = \mathcal{G}(p)$ which separates the percolating region (above) from the non-percolating (below) region. Three different critical curves are shown for $n = 2, 3$, and 4. The dependence of the critical fraction $v_c(p)$ on p for a specific value of n is obtained by the quadratic polynomial fit of the data as exhibited in Fig. 9:

$$v_c(p) = c_1 + c_2 p + c_3 p^2 \quad (6)$$

The values of c_1, c_2 , and c_3 are given in the Fig. 9 caption.

V. GENERALIZED COLORED PERCOLATION WITH SIMILAR AND DISSIMILAR BONDS

In this section we have generalized the model of colored percolation tuning the fractions of the bonds between similar and dissimilar colored atoms using two independent parameters. Specifically, for the site occupation probability $p > p_c$, the bonds between dissimilarly colored atoms are connected with probability u and those between similarly colored atoms are connected with probability v . Therefore, on the $u-v$ plane a critical percolation curve represents the phase boundary between the percolating and the non-percolating phases. In Fig. 10(a) we have shown for $n = 2$ and $q = 1/2$, a series of critical percolation curves for different values of occupation probability p . Here, the density of connected bonds is given by $\text{Prob}_b(u, v) = (u+v)/2$. The symmetry of this expression under the interchange of u and v is reflected by the mirror symmetry of the curves in Fig. 10(a) about the $v = u$ line. This can be generalized further for any

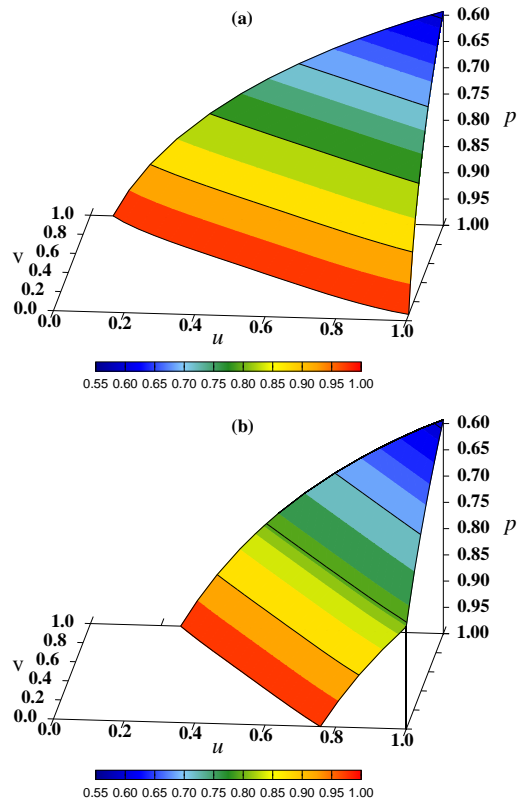


FIG. 11: 3D phase diagram has been drawn in the $u-v-p$ plane, for $n = 2$ (a) and $n = 3$ (b), with $q = 1/n$ using $L = 1024$ on the square lattice. The colored surface separates the percolating region from the non-percolating region.

value of n as $\text{Prob}_b(u, v) = u + (v - u)/n$, and therefore, for $n > 2$ the critical curves are not symmetric about the $u = v$ line any more. This has been exhibited in Fig. 10(b) for $n = 3$ and $q = 1/3$.

A better visualization of the percolating and non-percolating phases has been exhibited by a three-dimensional critical surface in the $(u-v-p)$ space. Fig. 11(a) and (b) exhibit such plots for $n = 2$ and 3 respectively. Any point within the space enclosed by the critical surface represents the percolating phase. The intersections of these critical surfaces with the $u = 1$ plane have been shown in Fig. 9 for $n = 2, 3$ and 4.

VI. UNIVERSALITY CLASS OF COLORED PERCOLATION

To confirm that the colored percolation belongs to the universality class of ordinary percolation, we have estimated a set of critical exponents, e. g., the fractal dimension of the largest cluster, the cluster size distribution exponent and the fractal dimension of the shortest paths right at the percolation threshold of the unpreffered colored percolation.

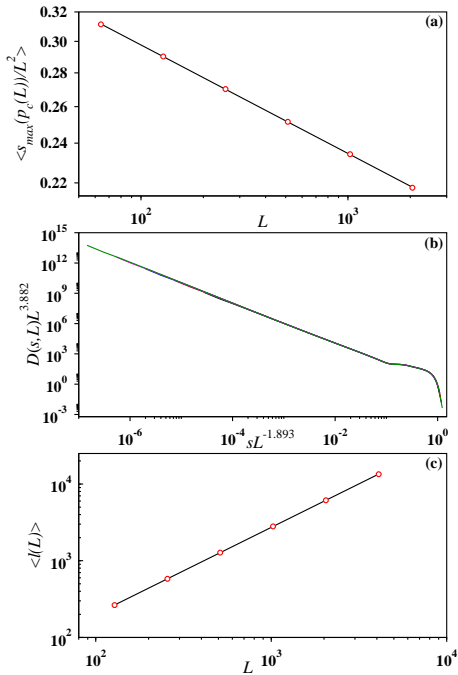


FIG. 12: Plots for $n = 3$ and $q = 1/3$ at the percolation threshold of the colored percolation on the square lattice. (a) The average fractional size $\langle s_{max}(p_c(L)) \rangle / L^2$ of the largest cluster plotted against the system size L gives a value of the fractal dimension $d_f = 1.897(2)$. (b) The finite-size scaling analysis of the cluster size distribution $D(s, L)$ has been exhibited. Plot of $D(s)L^{3.882}$ against $sL^{-1.893}$ shows an excellent data collapse, that yields $\tau = 2.051(5)$. (c) The average shortest path $\langle \ell(L) \rangle$ has been plotted against L for $L = 128, 256, 512, 1024, 2048$, and 4096 . The fractal dimension of the shortest path is estimated from the slope as $d_\ell = 1.133(2)$.

Fractal dimension: The average fractional size of the largest cluster at the percolation threshold decreases with the system size L as $\langle s_{max}(p_c(L)) \rangle / L^2 \sim L^{d_f-2}$, where d_f is its fractal dimension [41]. Our estimated values of $d_f = 1.897(2)$ for $n = 3$ on square lattice (Fig. 12(a)) and $1.895(2)$ for $n = 2$ on triangular lattice are compared with the fractal dimension $91/48 \approx 1.8958$ of the ordinary percolation in two dimensions.

Cluster Size Distribution: The size s of a percolation cluster being the number of occupied sites in the cluster. Cluster sizes are measured for all clusters right at the percolation threshold, marked by the maximal jump of the largest cluster. The cluster size distribution $D(s)$ is measured by averaging over many different configurations. In Fig. 12(b), the finite-size scaling of the data for $D(s)$ has been shown for $n = 3$ on the square lattice. An excellent collapse of the data confirms a power law variation: $D(s) \sim s^{-\tau}$. Using the best fitted values of the scaling exponents, the cluster size distribution exponent τ has been estimated to be $2.051(5)$, compared to $187/91 \approx 2.055$ for ordinary percolation in two dimensions [5, 43]. A very similar value of $2.051(5)$ has been

found for $n = 2$ on the triangular lattice.

Shortest Path: In general on a cluster, there exists multiple paths between an arbitrary pair of sites. The smallest of these is called the shortest path and its length is measured by the number ℓ of connected bonds on this path. Using the Burning algorithm [40] the average lengths $\langle \ell(n, L) \rangle$ of the system spanning shortest paths at the percolation threshold have been estimated and is found to scale with the lattice size L as $\langle \ell(n, L) \rangle \sim L^{d_\ell}$, with $d_\ell = 1.133(2)$ for $n = 3$ on the square lattice (Fig. 12(c)) and $1.133(3)$ for $n = 2$ on the triangular lattice compared to ≈ 1.131 in two dimension for the ordinary percolation [44, 45].

The same set of critical exponents have been estimated for the preferential colored percolation with $q = 0.60$ and we have obtained very similar matching with the exponents of ordinary percolation.

VII. SUMMARY

To summarize, we have introduced the model of ‘Colored Percolation’ and have formulated its infinite number of versions in two dimensions. The sites of a regular lattice are occupied by atoms with probability p and are colored randomly using one of the n distinct colors with probability $q = 1/n$. A bond is said to be connected if and only if its end atoms are of different colors. The global connectivity is then determined through the connected bonds. It has been observed that the percolation threshold $p_c(n)$ approaches p_c in the limit of $n \rightarrow \infty$ as $1/n$.

The preferential colored percolation has been defined when m out of n colors are selected with probability q/m each and rest of the colors are selected with probability $(1 - q)/(n - m)$. It has been observed that $p_c(q, m)$ depends non-trivially on q and has a minimum at $q_{min} = m/n$. The plot of $p_c(q, m)$ against q is asymmetric for general value of m , but it becomes symmetric about $q = 1/2$ only when $m = n/2$.

This model is further generalized by adding similarly colored bonds of density v . It has been found that for each value of the site occupation probability p , there exists a non-trivial value of $v_c(p)$. The phase diagram in the $v-p$ plane has been drawn with $v = v_c(p)$ as the critical curve separating the percolating and non-percolating regions. Such a phase diagram is better viewed in 3D and drawn by tuning v as well as u of the fraction of dissimilarly colored bonds and plotting the site occupation probability p along the z -axis. Estimation of different critical exponents lead us to conclude that all versions of the model of colored percolation belong to the percolation universality class.

VIII. ACKNOWLEDGMENTS

We gratefully acknowledge R. M. Ziff and D. Dhar for their useful comments on this work.

-
- [1] D. Stauffer and A. Aharony, *Introduction to Percolation Theory*, Taylor & Francis, (2003).
 - [2] G. Grimmett, *Percolation*, Springer (1999).
 - [3] R. Meester and R. Roy, *Continuum Percolation*, Cambridge University Press, (1996).
 - [4] M. Sahimi, *Applications of Percolation Theory*, Taylor & Francis, 1994.
 - [5] M. B. Isichenko, Rev. Mod. Phys. **64**, 961 (1992).
 - [6] M. Sahimi, Rev. Mod. Phys. **65**, 1393 (1993).
 - [7] S. Broadbent and J. Hammersley, *Percolation processes I. Crystals and mazes*, Proceedings of the Cambridge Philosophical Society **53**, 629 (1957).
 - [8] D. Sornette, *Critical Phenomena in Natural Sciences: Chaos, Fractals, Selforganization and Disorder: Concepts and Tools*, Springer (2006).
 - [9] N. Araujo, P. Grassberger, B. Kahng, K. J. Schrenk and R. M. Ziff, Eur. Phys. J. Special Topics **223**, 2307 (2014).
 - [10] A. A. Saberi, Physics Reports **578**, 1 (2015).
 - [11] D. Lee, Y. S. Cho and B. Kahng, J. Stat. Mech. **2016**, 124002 (2016).
 - [12] P. Santi, ACM Computing Surveys **37**, 164 (2005).
 - [13] D. Achlioptas, R. M. D'Souza, and J. Spencer, Science **323**, 1453 (2009).
 - [14] S. S. Manna and A. Chatterjee, Physica A **390**, 177 (2011).
 - [15] H. Hinrichsen, Adv. Phys. **49**, 815 (2000).
 - [16] F. Morone and H. A. Makse, Nature **524**, 65 (2015).
 - [17] A. Coniglio, H.E. Stanley and W. Klein, Phys. Rev. Lett. **42**, 518 (1979).
 - [18] L. de Arcangelis, S. Redner and H. J. Herrmann, J. Physique Lett. **46**, L585 (1985).
 - [19] G. G. Batrouni, A. Hansen and B. Larson, Phys. Rev. E **53**, 2292 (1996).
 - [20] T. Beer and I. G. Enting, Mathematical and Computer Modelling **13**, 77 (1990).
 - [21] M. E. J. Newman, Phys. Rev. E **66**, 016128 (2002).
 - [22] T. Tome and R. M. Ziff, Phys. Rev. E **82**, 051921 (2010).
 - [23] J. L. Jacobsen, J. Phys. A: Math. Theor., **48**, 454003 (2015).
 - [24] A complete list of percolation thresholds is in en.wikipedia.org/wiki/Percolation_threshold.
 - [25] M. Barma and J.W. Halley, *Infinite clusters in quenched AB alloys*, Nucl. Phys. and Solid State Phys. Symposium (India) **22C**, 493 (1979).
 - [26] T. Mai and J. W. Halley in *Ordering in two dimensions*, Elsevier North Holland, Inc., p-369 (1980).
 - [27] J. C. Wierman, Combinations and Graph Theory, **25**, 241 (1989).
 - [28] M. J. Appel, and J. C. Wierman, J. Phys. A **20**, 2527 (1987).
 - [29] X. Y. Wu and S. Y. Popov, J. Stat. Phys. **110**, 443 (2003).
 - [30] J. C. Wierman, and M. J. Appel, J. Phys. A **20**, 2533 (1987).
 - [31] F. Sevsek, J. M. Debierre and L. Turban, J. Phys. A **16**, 801 (1983).
 - [32] H. Nakanishi, J. Phys. A **20**, 6075 (1987).
 - [33] M. K. Wilkinson, J. Phys. A **20**, 3011 (1987).
 - [34] R. Zallen, Phys. Rev. B **16**, 1426 (1977).
 - [35] J. W. Halley, in: G. Deutscher, R. Zallen and J. Adler (eds) *Percolation Structures and Processes*, Adam Hilger, Bristol, p-323 (1983).
 - [36] S. Kundu and S. S. Manna, Phys. Rev. E, **93**, 062133 (2016).
 - [37] A. Margolina, H. J. Herrmann and D. Stauffer, Phys. Lett. **93A**, 73 (1982).
 - [38] M. E. J. Newman and R. M. Ziff, Phys. Rev. Lett. **85**, 4104 (2000).
 - [39] P. D. Eschbach, D. Stauffer and H. J. Herrmann, Phys. Rev. B, **23**, 422 (1981).
 - [40] H. J. Herrmann, D. C. Hong and H. E. Stanley, J. Phys. A **17**, L261 (1984).
 - [41] J. Feder, *Fractals*, Springer (1988).
 - [42] R. M. Ziff, Phys. Rev. E **82**, 051105 (2010).
 - [43] D. Stauffer, Phys. Rep., **54**, 2 (1979).
 - [44] Z. Zhou, J. Yang, Y. Deng and R. M. Ziff, Phys. Rev. E, **86**, 061101 (2012).
 - [45] K. J. Schrenk, N. Pose, J. J. Kranz, L. V. M. van Kessenich, N. A. M. Araujo and H. J. Herrmann, Phys. Rev. E, **88**, 052102 (2013).